Hindawi
Advances in Civil Engineering
Volume 2019, Article ID 8912390, 10 pages
https://doi.org/10.1155/2019/8912390

Research Article

Improving the Structural Reliability of Steel Frames Using Posttensioned Connections

Edén Bojórquez,[1] **Arturo López-Barraza**,[1] **Alfredo Reyes-Salazar**,[1] **Sonia E. Ruiz**,[2] **Jorge Ruiz-García**,[3] **Antonio Formisano**,[4] **Francisco López-Almansa**,[5] **Julián Carrillo**,[6] **and Juan Bojórquez**[1]

[1]*Facultad de Ingeniería, Universidad Autónoma de Sinaloa, Culiacán 80040, Mexico*
[2]*Instituto de Ingeniería, Universidad Nacional Autónoma de México, México City 04510, Mexico*
[3]*Facultad de Ingeniería Civil, Universidad Michoacana de San Nicolás de Hidalgo, Morelia 58040, Mexico*
[4]*Department of Structures for Engineering and Architecture (DiSt), University of Naples "Federico II", Naples 80125, Italy*
[5]*Architecture Technology Department, Technical University of Catalonia, Barcelona 08028, Spain*
[6]*Ingeniería Civil, Universidad Militar Nueva Granada, Bogotá, Colombia*

Correspondence should be addressed to Edén Bojórquez; eden@uas.edu.mx

Received 23 March 2019; Accepted 2 June 2019; Published 26 June 2019

Academic Editor: Rosario Montuori

In this paper, various moment-resisting steel frames (MRSFs) are subjected to 30 narrow-band motions scaled at different ground motion intensity levels in terms of spectral acceleration at first mode of vibration $S_a(T_1)$ in order to perform incremental dynamic analysis for peak and residual interstory drift demands. The results are used to compute the structural reliability of the steel frames by means of hazard curves for peak and residual drifts. It is observed that the structures exceed the threshold residual drift of 0.5%, which is perceptible to human occupants, and it could lead to human discomfort according to recent investigations. For this reason, posttensioned connections (PTCs) are incorporated into the steel frames in order to improve the structural reliability. The results suggest that the annual rate of exceedance of peak and residual interstory drift demands are reduced with the use of PTC. Thus, the structural reliability of the steel frames with PTC is superior to that of the MRSFs. In particular, the residual drift demands tend to be smaller when PTCs are incorporated in the steel structures.

1. Introduction

Currently, most of the seismic design regulations recommend the use of maximum interstory drift as the main engineering demand parameter. Nevertheless, earthquake field reconnaissance has evidenced that residual drift demands after an earthquake play an important role in the seismic performance of a structure. For example, several dozen damaged reinforced concrete structures in Mexico City had to be demolished after the 1985 Michoacan earthquake because of the technical difficulties to straighten and to repair buildings with large permanent drifts [1]. Okada et al. [2] reported that several low-rise RC buildings suffered light structural damage but experienced relatively large residual deformations as a consequence of the 1995 Hyogo-Ken Nambu earthquake even though they had sufficient deformation capacity. After examining 12 low-to-mid-rise steel office buildings (particularly 10 with structural system based on steel moment-resisting frames) structurally damaged and leaned after the same earthquake, Iwata et al. [3] highlighted that the cost of repair of leaned steel buildings linearly increased as the maximum and roof residual drift increased. Based on their study, the authors suggested that steel buildings should be limited to maximum and roof residual drift about 1.4% and 0.9%, respectively, to satisfy a repairability limit state that meets both technical and economical constraints. More recently, a field investigation in Japan indicated that a residual interstory drift of about 0.5% is perceptible for building occupants [4]. Bojórquez and Ruiz-García [5] by comparing peak and residual drift demand hazard curves have observed that if steel

frames exhibit peak drift demands about 3%, they could experience residual drifts larger than 0.5%, which is the threshold residual drift that could be tolerable to human occupants, and it could lead to human discomfort [4] when subjected to narrow-band earthquake ground motions of high intensity. Therefore, several researchers have demonstrated that the estimation of residual drift demands should also play an important role during the design of new buildings [6–8] and the evaluation of the seismic structural performance of existing buildings [9–13].

In the present study, motivated by the need to reduce peak and residual interstory drift demands, PTCs are incorporated into various MRSFs. Posttensioned steel moment-resisting frames are structural systems proposed in recent years as an appropriate alternative to welded connections of moment-resisting frames in seismic zones [14–27]. They are designed to prevent brittle fractures in the area of the nodes of steel frames, which can cause severe reduction in their ductility capacity, as occurred in many cases during the 1994 Northridge and the 1995 Kobe earthquakes. The philosophy of structures with PTC is that under an intense earthquake motion, beams and columns remain essentially elastic concentrating the damage on the energy dissipating elements, which can be easily replaced at low cost. Moreover, they provide capacity of energy dissipation and self-centering which can significantly reduce the residual demands. The structural performance of the selected MRSFs is compared with the structures with PTC through incremental dynamic analysis and the estimation of the structural reliability of the frames in terms of peak and residual interstory drift demands. With this aim, four MRSFs and the same structures with PTC (here named FPTC frames with posttensioned connections) are subjected to 30 long-duration ground motions recorded at the lake zone of Mexico City where most of the damages were found in buildings as a consequence of the 1985 Michoacan earthquake. In general, it is observed that the structural reliability of the steel frames with PTC is superior to that of the MRSFs. In particular, the residual drift demands tend to be smaller than 0.5% (which is perceptible for building occupants) when PTCs are incorporated into the steel structures.

2. Methodology

2.1. Structural Steel Frame Models. Two groups of four structural steel frame models are selected for the study. The first group of structures corresponding to moment-resisting steel frames was designed according to the Mexico City Building Design Provisions (MCSDPs) [28]. The buildings are assumed to be for office occupancy. They have 4, 6, 8, and 10 stories, and 3 bays, hereafter indicated as F4, F6, F8, and F10, respectively. The dimensions of the frames are shown in Figure 1. The beams and columns are A36 steel W sections. A bilinear hysteretic model for accounting the nonlinear material behavior with 3% of postyielding stiffness was considered for the analyses, and the damping used was 3% of critical. The fundamental periods of vibration (T_1) are 0.9, 1.07, 1.20, and 1.37 s, respectively. On the other hand, the FPTCs were designed in accordance with the recommendations proposed by Garlock et al. [21], which basically start

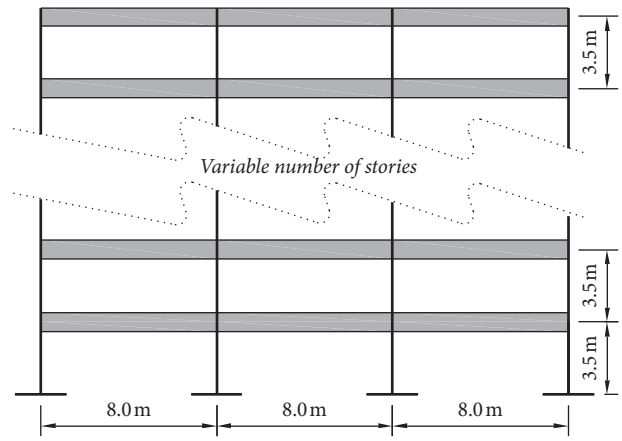

Figure 1: Geometrical characteristics of the MRSFs.

with the design of the steel frames as usually done (considering rigid connections), and then, the semirigid posttensioned connections are designed to satisfy the requirements of the serviceability and resistance conditions. The beam-column connections consist of two angles bolted to the flanges of the beam and to the column flange (top and seat). For the design of posttensioned connections, steel grade 50 was used for the angles. The length of the angles was taken equal to the width of the flange of the beams (b_f). Different angle sizes were tested, but at the end, $152 \times 152 \times 13$ mm angles were used in all the cases. Posttensioned cables consist of seven wires with an area of 150 mm^2, withstanding a load of 279 kN; they are parallel to the axis of the beam passing through the interior columns and fixed to the outer face of the columns at the ends of the frame. An initial tension of the cables less than 0.33 times their maximum capacity was used according with the suggestions given by Garlock et al. [21]. The four FPTC models are identified here as F4PTC, F6PTC, F8PTC, and F10PTC, for the frames with 4, 6, 8, and 10 stories, respectively. The FPTC models have fundamental periods of vibration of 0.89, 1.03, 1.25, and 1.37 s, respectively. The columns of the ground floor are fixed at the base without being posttensioned. The beam and column members used for all the frames are illustrated in Table 1. Note that the mechanical characteristics and dimensions of beams and columns are the same for both the MRSFs and FPTC. Figure 2 shows a typical assembly of a posttensioned steel frame.

2.2. Connection Model: Nonlinear Hysteretic Behavior. The hysteretic rules that represent the cyclic behavior of the semirigid connections of the posttensioned frames are characterized by moment-rotation curves (M-θ_r), with shapes similar to a flag. This representation characterizes the nonlinearity, self-centering capability, and energy dissipation capacity of the connection. Experimental tests with isolated angles, subjected to cyclic and monotonic loads, conducted by Shen and Astaneh-Asl [29] showed a stable cyclic response and good capability of hysteretic energy dissipation. In general, ultimate strength exceeded 3 times the yield strength, and ductility reached values between 8 and 10. The strength and stiffness in bending of the posttensioned connections is

Table 1: Relevant characteristics of the steel frames.

Frame	F4	F6	F8	F10
Number of stories	4	6	8	10
Internal columns				
Story 1	W21 × 122	W30 × 173	W36 × 210	W36 × 280
Story 2	W21 × 122	W30 × 173	W36 × 210	W36 × 280
Story 3	W21 × 111	W30 × 148	W36 × 194	W36 × 245
Story 4	W21 × 111	W30 × 148	W36 × 194	W36 × 245
Story 5		W30 × 124	W36 × 170	W36 × 210
Story 6		W30 × 124	W36 × 170	W36 × 210
Story 7			W36 × 160	W36 × 182
Story 8			W36 × 160	W36 × 182
Story 9				W36 × 150
Story 10				W36 × 150
External columns				
Story 1	W18 × 97	W27 × 146	W36 × 194	W36 × 280
Story 2	W18 × 97	W27 × 146	W36 × 194	W36 × 280
Story 3	W18 × 86	W27 × 129	W36 × 182	W36 × 245
Story 4	W18 × 86	W27 × 129	W36 × 182	W36 × 245
Story 5		W27 × 114	W36 × 160	W36 × 210
Story 6		W27 × 114	W36 × 160	W36 × 210
Story 7			W36 × 135	W36 × 182
Story 8			W36 × 135	W36 × 182
Story 9				W36 × 150
Story 10				W36 × 150
Beams				
Story 1	W16 × 67	W18 × 71	W21 × 83	W21 × 68
Story 2	W16 × 57	W18 × 76	W21 × 93	W21 × 93
Story 3	W16 × 45	W18 × 76	W21 × 93	W21 × 101
Story 4	W16 × 40	W16 × 67	W21 × 83	W21 × 101
Story 5		W16 × 50	W18 × 71	W21 × 101
Story 6		W16 × 45	W18 × 65	W21 × 93
Story 7			W18 × 55	W21 × 73
Story 8			W18 × 46	W21 × 68
Story 9				W21 × 57
Story 10				W21 × 50

provided by the contribution of the angles of the PTC and by posttensioned strands. Wires and angles work as springs in parallel. Posttensioned strands exhibit linear behavior, while connecting angles behave nonlinearly. Figure 3 shows a typical example of a hysteretic curve corresponding to a posttensioned connection. This behavior was modeled by mean of equations (1) and (2) which represent the loading and unloading curves, respectively, obtained from the superposition of the exponential equation proposed by Richard [30] for semirigid connections and the linear contribution of the strands, as well as decompression moments (M_d) and the closing moment (M_c) of the connection. The first function, given by equation (1), corresponds to the initial loading cycle; two types of variables are observed: (1) variables depending only on geometric and physical properties of angles, such as initial (k) and postyield (k_p) stiffnesses, the reference moment (M_o), and N that defines the curvature in the transition between the linear and plastic behavior and (2) variables depending on the number and type of tendons such as the rigidity of the posttensioned tendons ($k_{\theta S}$) and the bending moment associated with the opening of the connection (named decompression moment, M_d) which is a function of the resulting initial tension in the tendons. The second function, given by equation (2), defines the unloading and reloading process in the connection; M_a and θ_a are the maximum values reached in each cycle, and the parameter φ defines the magnitude of the closing moment of the connection (M_c), which must be greater than zero in order to insure complete closure of the connection after getting complete unloading; moreover, this parameter largely defines the E_H dissipation capacity of the connection (enclosed area). The curves obtained with the modified model exhibit good accuracy in comparison with experiment results, and they were modeled in RUAUMOKO [31] as the flag-shaped bilinear hysteresis [32].

$$M = M_d + \frac{\left(k - k_p\right)\theta_r}{\left[1 + \left|\left(\left(k - k_p\right)\theta_r\right)/M_o\right|^N\right]^{1/N}} + \left(k_p + k_{\theta S}\right)\theta_r, \tag{1}$$

$$M = M_a - \frac{\left(k - k_p\right)\left(\theta_a - \theta_r\right)}{\left[1 + \left|\left(\left(k - k_p\right)\left(\theta_a - \theta_r\right)\right)/\varphi M_o\right|^N\right]^{1/N}} - \left(k_p + k_{\theta S}\right)\left(\theta_a - \theta_r\right). \tag{2}$$

2.3. Earthquake Ground Motions. A total of 30 narrow-band earthquake ground motions recorded at soft soil sites of Mexico City are used for the time story analyses of the MSRF and FPTC. The main characteristic of the selected ground motions recorded on soft soils is that they demand large energy on structures in comparison to those recorded on firm soils [33, 34]. The ground motions were recorded in sites where the period of the soil was close to two seconds and structures were more severely damaged during the 1985 Mexico City Earthquake. The duration was computed according with Trifunac and Brady [35]. Table 2 summarizes the most important characteristics of the records. In the table, while PGA and PGV denote the peak ground acceleration and velocity, t_D indicates duration.

2.4. Evaluation of Structural Reliability. The incremental dynamic analysis [36] is used to assess the seismic performance of the steel frames under narrow-band motions at different intensity levels. Next, the well-known seismic performance-based assessment procedure suggested by the Pacific Earthquake Engineering Center [37] in the United States was employed in this study, which indicates that the mean annual frequency of exceedance of an engineering demand parameter (EDP) of interest exceeding a certain level EDP can be computed as follows:

$$\lambda\left(\mathrm{EDP} > \mathrm{edp}\right) \cong \int_{\mathrm{IM}} P\left[\mathrm{EDP} > \mathrm{edp} \mid \mathrm{IM} = \mathrm{im}\right] \cdot \left|d\lambda_{\mathrm{IM}}\left(\mathrm{im}\right)\right|, \tag{3}$$

where IM denotes the ground motion intensity measure (e.g., peak ground acceleration, spectral acceleration at the

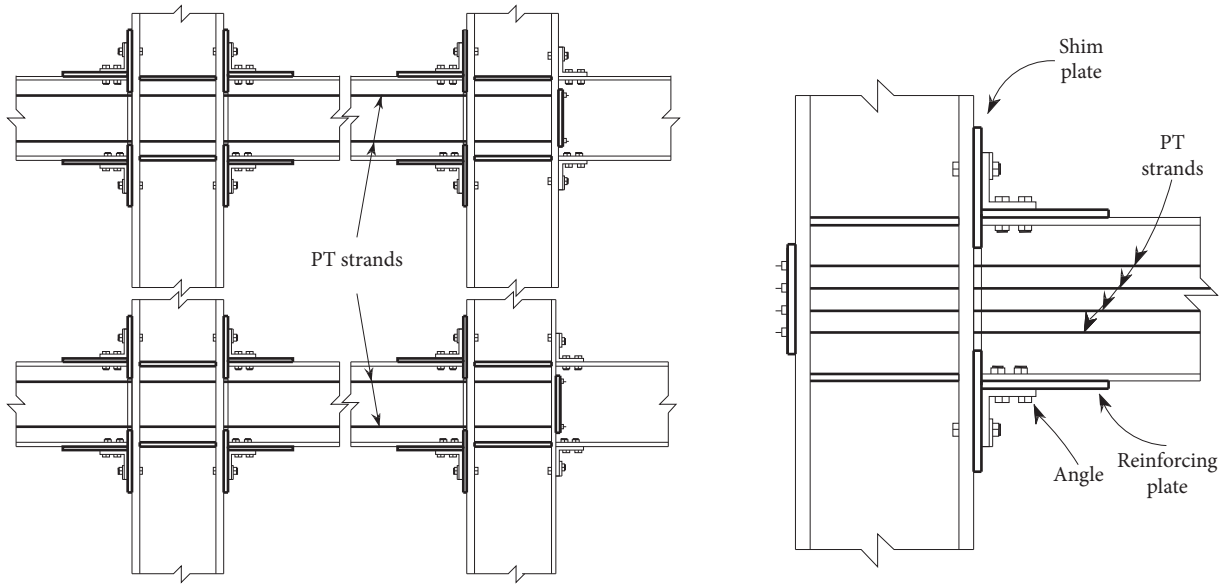

Figure 2: Angles and posttensioned strands in the FPTC structures.

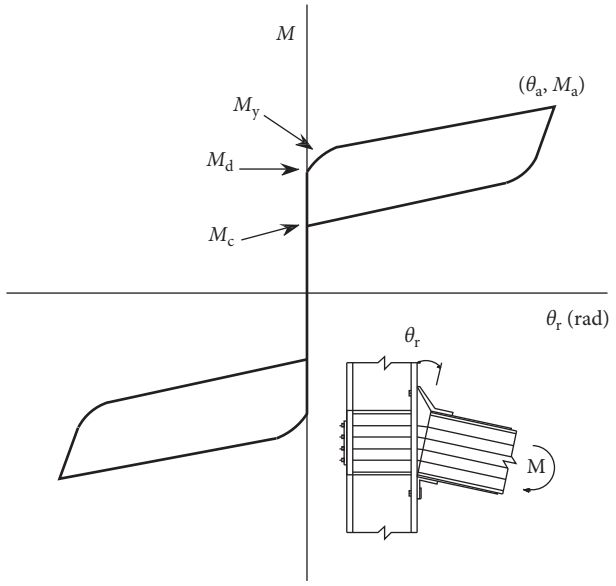

Figure 3: Moment-relative rotation hysteretic curve for the posttensioned connections.

first-mode period of vibration, and inelastic displacement demand at the building's fundamental period of vibration) and $P[\mathrm{EDP} > \mathrm{edp} \mid \mathrm{IM} = \mathrm{im}]$ is the conditional probability that an EDP exceeds a certain level of EDP given that the IM is evaluated at the ground motion intensity measure level im. In addition, $d\lambda_{\mathrm{IM}}(\mathrm{im})$ refers to the differential of the ground motion hazard curve for the IM. In this context, while the first term in the right-hand side of equation (3) can be obtained from probabilistic estimates of the EDP of interest with incremental dynamic analyses, the second term in equation (3) is represented by the seismic hazard curve, which can be computed from conventional Probabilistic Seismic Hazard Analysis (PSHA), evaluated at the ground motion intensity level im. Note the importance of the ground motion intensity measure for assessment of seismic performance, which is the joint between earthquake engineering and seismology. In this study, the spectral acceleration at first mode of vibration $S_a(T_1)$ was selected as IM, in such a way that equation (3) can be expressed as

$$\lambda(\mathrm{EDP} > \mathrm{edp}) \cong \int_{S_a(T_1)} P\left[\mathrm{EDP} > \mathrm{edp} \mid S_a(T_1) = s_a\right] \cdot \left|d\lambda_{S_a(T_1)}(s_a)\right|, \tag{4}$$

where $d\lambda_{S_a(T_1)}(s_a) = \lambda_{S_a(T_1)}(s_a) - \lambda_{S_a(T_1)}(s_a + ds_a)$ is the hazard curve differential expressed in terms of $S_a(T_1)$. Equation (4) was used to evaluate the structural reliability of the study-case frames in terms of two EDPs: peak and residual interstory drift demands. For evaluating the first term in the integrand for peak and residual drift demands, a lognormal cumulative probability distribution was used [5]. Therefore, the term $P(\mathrm{EDP} > \mathrm{edp} \mid S_a(T_1) = s_a)$ is analytically evaluated as follows:

$$P\left(\mathrm{EDP} > \mathrm{edp} \mid S_a(T_1) = s_a\right) = 1 - \Phi\left(\frac{\ln \mathrm{edp} - \widehat{\mu}_{\ln\mathrm{EDP}\mid S_a(T_1)=s_a}}{\widehat{\sigma}_{\ln\mathrm{EDP}\mid S_a(T_1)=s_a}}\right), \tag{5}$$

where $\widehat{\mu}_{\ln\mathrm{EDP}\mid S_a(T_1)=s_a}$ and $\widehat{\sigma}_{\ln\mathrm{EDP}\mid S_a(T_1)=s_a}$ are the geometric mean and standard deviation of the natural logarithm of the EDP, respectively, and $\Phi(\cdot)$ is the standard normal cumulative distribution function. It is important to say as Bojórquez et al. [38] indicate that the ground motion records used in the present study allow the use of spectral acceleration at first mode of vibration as intensity measure due to its sufficiency with respect to magnitude and distance and because of the similarity of the spectral shape of the records since they have similar values of the spectral parameter N_p [39].

2.5. Seismic Performance in terms of Peak and Residual Drift Demands: MRSFs vs Steel Frames with PTC. The first step to

Table 2: Narrow-band motions used for the present study.

Record	Date	Magnitude	Station	PGA (cm/s^2)	PGV (cm/s)	t_D (s)
1	19/09/1985	8.1	SCT	178.0	59.5	34.8
2	21/09/1985	7.6	Tlahuac deportivo	48.7	14.6	39.9
3	25/04/1989	6.9	Alameda	45.0	15.6	37.8
4	25/04/1989	6.9	Garibaldi	68.0	21.5	65.5
5	25/04/1989	6.9	SCT	44.9	12.8	65.8
6	25/04/1989	6.9	Sector popular	45.1	15.3	79.4
7	25/04/1989	6.9	Tlatelolco TL08	52.9	17.3	56.6
8	25/04/1989	6.9	Tlatelolco TL55	49.5	17.3	50.0
9	14/09/1995	7.3	Alameda	39.3	12.2	53.7
10	14/09/1995	7.3	Garibaldi	39.1	10.6	86.8
11	14/09/1995	7.3	Liconsa	30.1	9.62	60.0
12	14/09/1995	7.3	Plutarco Elías Calles	33.5	9.37	77.8
13	14/09/1995	7.3	Sector popular	34.3	12.5	101.2
14	14/09/1995	7.3	Tlatelolco TL08	27.5	7.8	85.9
15	14/09/1995	7.3	Tlatelolco TL55	27.2	7.4	68.3
16	09/10/1995	7.5	Cibeles	14.4	4.6	85.5
17	09/10/1995	7.5	CU Juárez	15.8	5.1	97.6
18	09/10/1995	7.5	Centro urbano Presidente Juárez	15.7	4.8	82.6
19	09/10/1995	7.5	Córdoba	24.9	8.6	105.1
20	09/10/1995	7.5	Liverpool	17.6	6.3	104.5
21	09/10/1995	7.5	Plutarco Elías Calles	19.2	7.9	137.5
22	09/10/1995	7.5	Sector popular	13.7	5.3	98.4
23	09/10/1995	7.5	Valle Gómez	17.9	7.18	62.3
24	11/01/1997	6.9	CU Juárez	16.2	5.9	61.1
25	11/01/1997	6.9	Centro urbano Presidente Juárez	16.3	5.5	85.7
26	11/01/1997	6.9	García Campillo	18.7	6.9	57.0
27	11/01/1997	6.9	Plutarco Elías Calles	22.2	8.6	76.7
28	11/01/1997	6.9	Est. # 10 Roma A	21.0	7.76	74.1
29	11/01/1997	6.9	Est. # 11 Roma B	20.4	7.1	81.6
30	11/01/1997	6.9	Tlatelolco TL08	16.0	7.2	57.5

evaluate the structural reliability is the computation of the incremental dynamic analysis; thus, the maximum or residual interstory drift at different values of the ground motion intensity measure which in the present study is $S_a(T_1)$ is calculated. Figure 4 illustrates as an example the incremental dynamic analysis of the traditional frame F4 under the selected narrow-band motions. It can be observed the increase of the maximum interstory drift as the spectral acceleration at first mode of vibration tends to increase. Likewise, notice that the uncertainty in the structural response also tend to increase for larger values of $S_a(T_1)$. Then, the fragility curves are computed through equation (5), which are combined with the seismic hazard curves to compute the mean annual rate of exceedance, thus the structural reliability via equation (4) in terms of peak and residual interstory drift. Note that in this case, the spectral acceleration hazard curves corresponding to the first-mode period of vibration of each building and for the *Secretaría de Comunicaciones y Transportes* (SCT) site in Mexico City were developed following the procedure suggested by Alamilla [40].

The Mexican City seismic design code takes into account the peak interstory drift. Recently, Bojórquez and Ruiz-García [5] demonstrated that, for MRSFs designed with the Mexican City Building Code, the control of maximum or peak interstory drift demands does not necessarily guarantee a good seismic performance in terms of residual drift demands. In fact, by comparing peak and residual drift demand hazard curves, Bojórquez and Ruiz-García [5] concluded that, for steel structures that exhibit peak drift demands of about 3% (the threshold recommended by the MCSDP to avoid collapse), the maximum residual drifts is larger than 0.5%, which is the threshold residual drift that could be tolerable to human occupants, and it could lead to human discomfort identified from recent field investigations [4] when subjected to narrow-band earthquake ground motions of high intensity. For this reason, the residual interstory drift should be considered in future versions of the

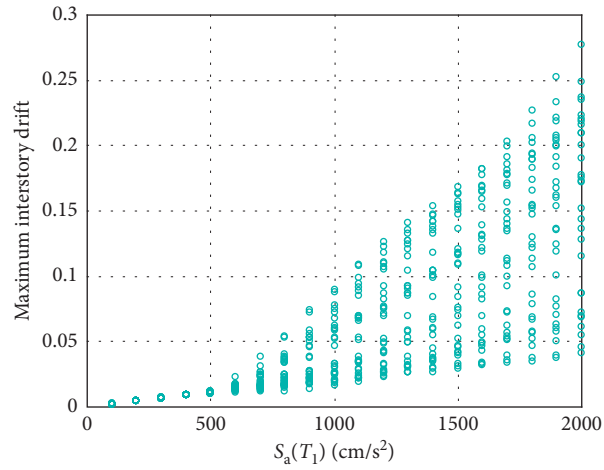

Figure 4: Incremental dynamic analysis of frame F4.

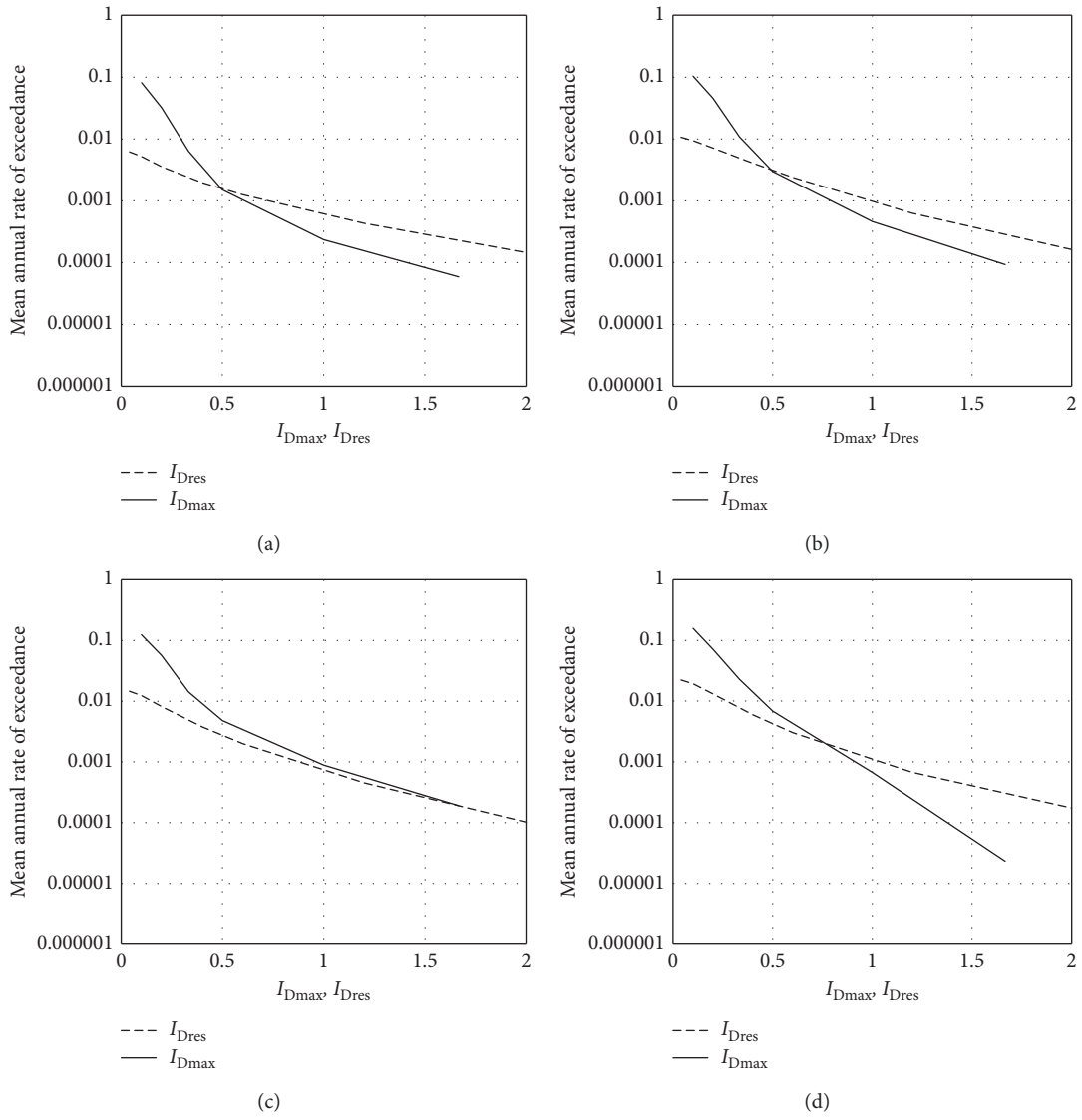

Figure 5: Comparison of the I_{Dmax} and I_{Dres} hazard curves for the MRSFs: (a) F4, (b) F6, (c) F8, and (d) F10.

Mexican Building Code to guarantee an adequate structural dynamic behavior of buildings prone to earthquakes. To further illustrate the importance of residual drift demands in comparison with peak interstory drift demands via seismic analysis. Two damage indicators are computed. The first damage parameter is calculated as the ratio of the maximum interstory drift demand divided by 3%, the threshold value of maximum drift to avoid collapse according to the MCBC, in such a way that values equal to or larger than one of this maximum drift damage index (I_{Dmax}) indicates the failure of the system in terms of peak drift. On the other hand, the second damage index I_{Dres} is similar to the first one but the residual peak drift demand divided by a value of 0.5% should be considered (the threshold residual drift limit that could be perceptible to human occupants and it could lead to human discomfort [4]). Values larger than one of I_{Dres} are related to the structural failure in terms of residual demands. Figure 5 compares the I_{Dmax} and I_{Dres} hazard curves for all the MRSFs at different performance levels. It is observed that in the case of the frames F4, F6, F8, and F10, when the damage index is equals to one, the mean annual rate of exceedance (MARE) is smaller in terms of peak interstory drift demands in comparison with the residual drift. In other words, the structural reliability of the selected MRSFs is larger for peak drifts indicating that the control of maximum demand does not necessarily guarantee the same level of safety in terms of residual drift demands. For this reason, if the parameter to estimate the structural performance of structures is the maximum interstory drift demand, it is necessary to obtain larger structural reliability levels aimed to provide adequate structural performance in terms of residual drift because it is necessary to obtain at least the same structural reliability in terms of I_{Dmax} and I_{Dres}. For this reason, with the aim to increase the seismic performance for residual drift demands, PTCs are incorporated in the selected MRSFs.

The seismic hazard curves in terms of maximum interstory drift damage index I_{Dmax} obtained for the MRSFs and the PTC steel frames are compared in Figure 6. In this

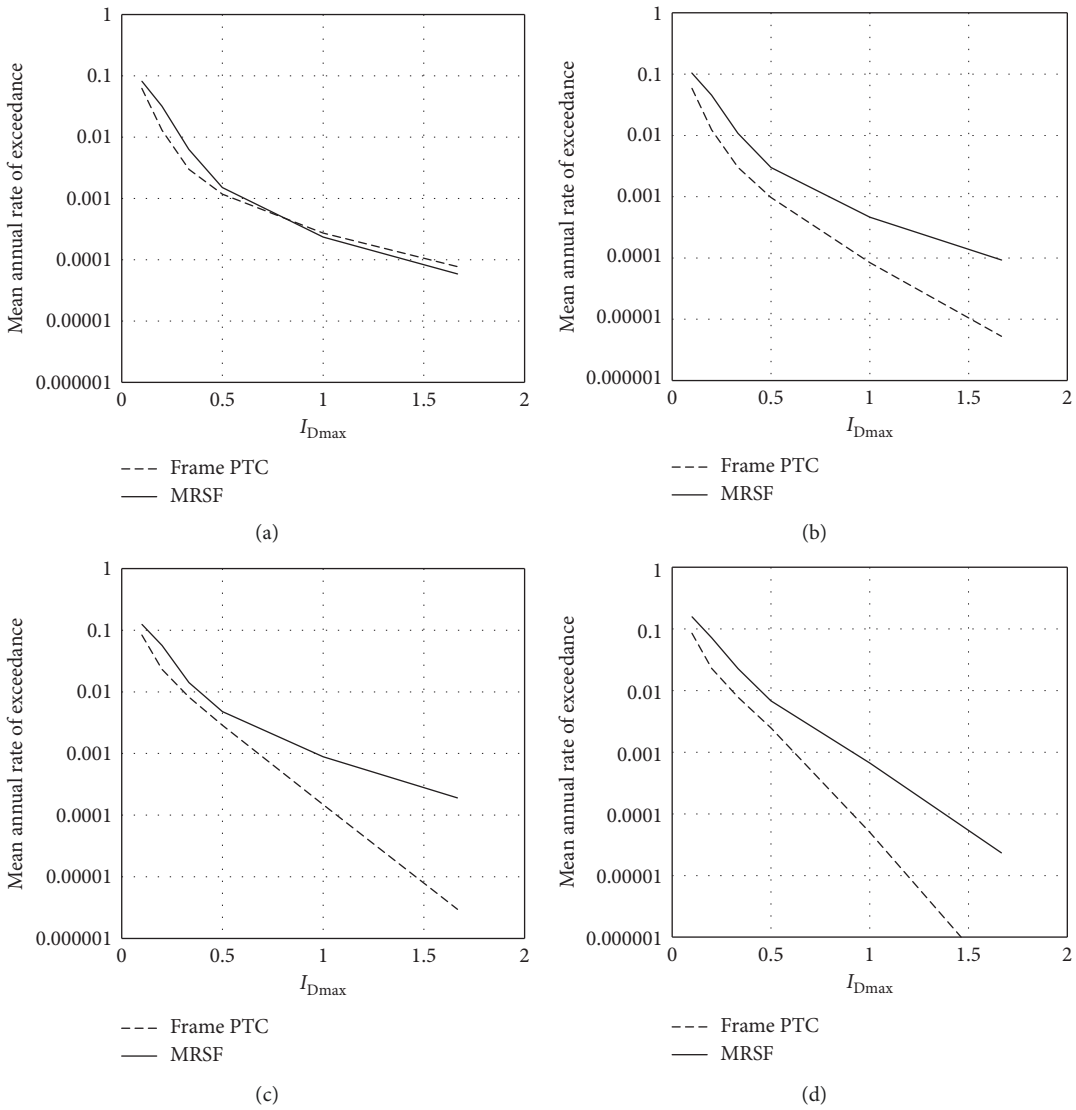

FIGURE 6: Comparison of the I_{Dmax} curves for the MRSFs and the PTC steel frames with (a) 4 stories, (b) 6 stories, (c) 8 stories, and (d) 10 stories.

figure, it can be observed that the structural reliability or the mean annual rate of exceeding a specific value of maximum interstory drift is in general smaller for the steel frame with PTC. Thus, the seismic performance in terms of peak demands is increasing when the PTCs are incorporated in the traditional MRSFs, which also could represent an increase in the structural reliability for the residual interstory drift demands as will be discussed below.

The comparison of the structural reliability for the MRSFs and the PTC frames in terms of residual drift demands provided by the I_{Dres} (damage index in terms of residual displacements) is illustrated in Figure 7. As it was expected, the mean annual rate of exceedance of I_{Dres} value is reduced when PTCs are incorporated into the traditional steel frames, which is valid for all the structures under consideration. In such a way, the use of PTC is a good alternative, for example, as a solution for rehabilitation of buildings or in order to reduce peak and residual drift demands of traditional structural steel systems under severe earthquakes.

Finally, a comparison of the mean annual rate of exceedance values when the damage index is equal to one in terms of I_{Dmax} for the MRSFs and in terms of I_{Dres} for the PTC steel frames is provided in Table 3. The aim of using the MARE values for I_{Dmax} is because they represent the target structural reliability levels obtained buildings designed according to the Mexican Building Code. Thus, the MARE values in terms of I_{Dres} for the PTC steel frames should be reduced in comparison to those of peak interstory drift for the MRSFs to guarantee that by including PTC in the traditional steel frames, it is possible to satisfy the structural reliability for the residual demands provided by the requirements of the Mexican Code. In Table 3, a column name ratio was used which represents the ratio of MARE of I_{Dres} (PTC steel frames) divided by I_{Dmax} (MRSFs), and values

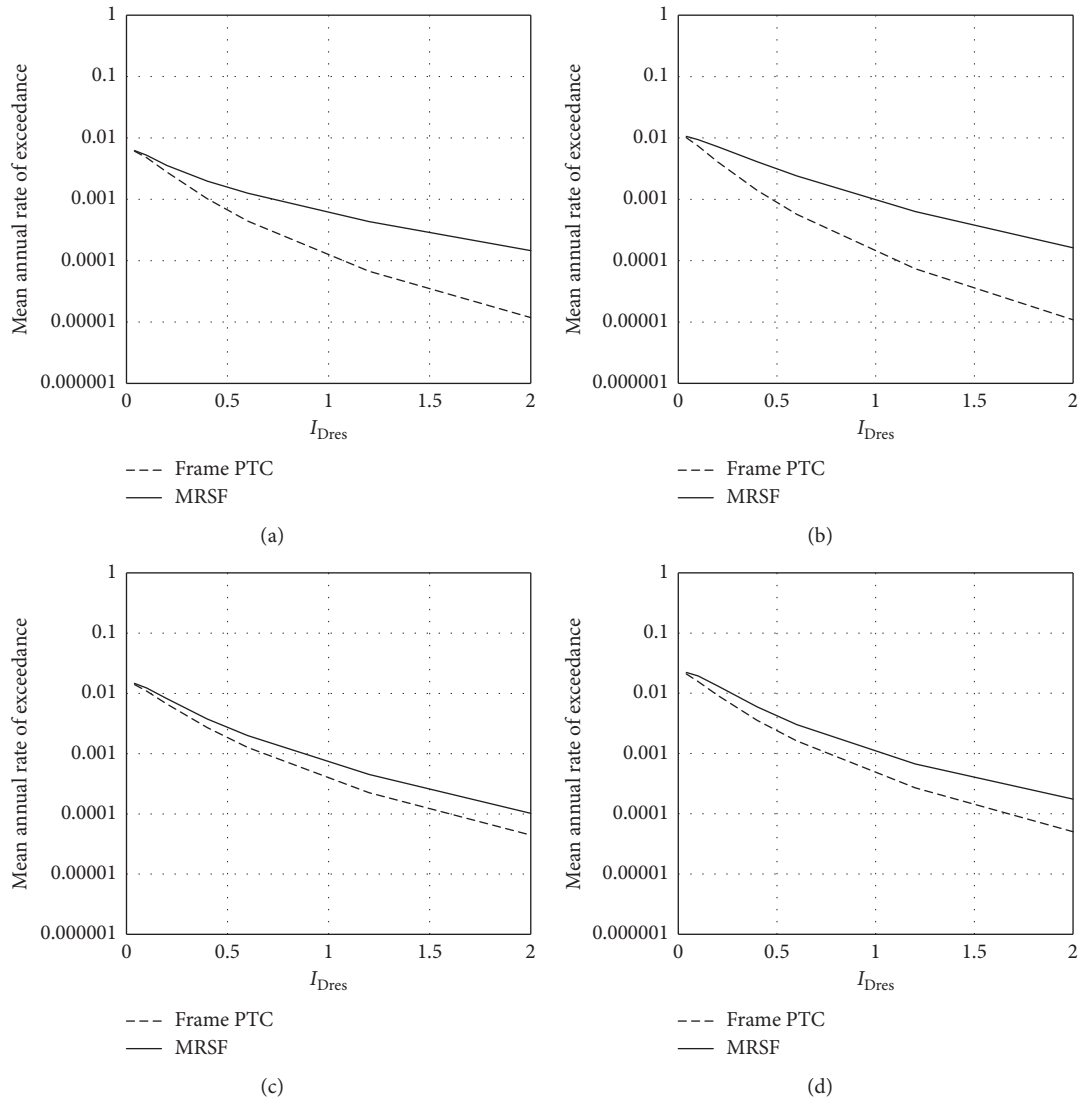

Figure 7: Comparison of the I_{Dres} hazard curves for the MRSFs and the PTC steel frames with (a) 4 stories, (b) 6 stories, (c) 8 stories, and (d) 10 stories.

Table 3: Mean annual rate of exceedance values when the damage index is equal to one in terms of I_{Dmax} for the MRSFs and in terms of I_{Dres} for the PTC steel frames.

Steel frame	MARE for $I_{Dmax} = 1$	Steel frame	MARE for $I_{Dres} = 1$	Ratio
F4	0.00024	F4	0.00019	0.79
F6	0.00046	F6	0.00024	0.52
F8	0.00089	F8	0.00057	0.64
F10	0.00067	F10	0.00072	1.07

smaller or equal to one indicates that the structural reliability is larger in terms of residual drift demands for the PTC frames comparing with the peak drifts of the MRSFs. It is observed that the values of the mean annual rates of exceedance for the PTC steel frames are in general smaller to those of the traditional structures when the damage index is equal to one.

3. Conclusions

The structural reliability of four moment-resisting steel frames is estimated in terms of peak and residual interstory drift seismic demands. For this aim, all the structures are subjected to 30 narrow-band ground motion records of the soft soil of Mexico City. The numerical results indicates that the structural reliability of the traditional steel frames is not adequate in terms of residual interstory drift demands. For this reason, PTCs are incorporated into the selected steel framed buildings in order to increase the structural reliability based on a damage index for the residual interstory drifts. As it was expected, for most of the steel framed buildings, the ability of self-centering for the steel frames incorporating PTC reduces significantly the residual demands; in fact, for this type of structural systems, the structural reliability is larger in terms of residual interstory drifts for most of the frames under consideration in comparison with peak demands of the

MRSFs. Moreover, the seismic performance in terms of peak demands is also increasing when PTCs are incorporated into the traditional MRSFs. It is concluded that the use of PTC is a good alternative as a solution for rehabilitation of buildings or in order to reduce peak and residual interstory drift seismic demands of traditional structural steel systems under severe earthquakes. Furthermore, PTC in steel frames could be an interesting solution toward structural systems with high seismic resilience.

Data Availability

The data used to support the findings of this study are available from the corresponding author upon request.

Conflicts of Interest

The authors declare that there are no conflicts of interest regarding the publication of this paper.

Acknowledgments

The financial support given by the Universidad Autónoma de Sinaloa under grant PROFAPI and the Universidad Michoacana de San Nicolás de Hidalgo is appreciated. The authors express their gratitude to the *Consejo Nacional de Ciencia y Tecnología* (CONACYT) in Mexico for funding the research reported in this paper under grant Ciencia Básica. Financial support also was given by DGAPA-UNAM under grant PAPIIT IN10351. In addition, Julián Carrillo thanks the Vicerrectoría de Investigaciones at Universidad Militar Nueva Granada for providing research grants.

References

[1] E. Rosenblueth and R. Meli, "The 1985 Mexico earthquake: causes and effects in Mexico City," *Concrete International (ACI)*, vol. 8, no. 5, pp. 23–34, 1986.

[2] T. Okada, T. Kabeyasawa, T. Nakano, M. Maeda, and T. Nakamura, "Improvement of seismic performance of reinforced concrete school buildings in Japan-Part 1 Damage survey and performance evaluation after the 1995 Hyogo-Ken Nambu earthquake," in *Proceedings of the 12th World Conference on Earthquake Engineering*, vol. 2421, Auckland, New Zealand, February 2000.

[3] Y. Iwata, H. Sugimoto, and H. Kuguamura, "Reparability limit of steel structural buildings based on the actual data of the Hyogoken-Nanbu earthquake," in *Proceedings of the 38th Joint Panel*, vol. 1057, pp. 23–32, Wind and Seismic effects, NIST Special Publication, Gaithersburg, MD, USA, May 2006.

[4] J. McCormick, H. Aburano, M. Ikenaga, and M. Nakashima, "Permissible residual deformation levels for building structures considering both safety and human elements," in *Proceedings of the 14th World Conference on Earthquake Engineering*, Beijing, China, October 2008.

[5] E. Bojórquez and J. Ruiz-García, "Residual drift demands in moment-resisting steel frames subjected to narrow-band earthquake ground motions," *Earthquake Engineering and Structural Dynamics*, vol. 42, no. 11, pp. 1583–1598, 2013.

[6] S. Pampanin, C. Christopoulos, and M. J. Nigel Priestley, "Performance-based seismic response of frame structures including residual deformations: part II: multi-degree of freedom systems," *Journal of Earthquake Engineering*, vol. 7, no. 1, pp. 119–147, 2003.

[7] D. Pettinga, C. Christopoulos, S. Pampanin, and N. Priestley, "Effectiveness of simple approaches in mitigating residual deformations in buildings," *Earthquake Engineering & Structural Dynamics*, vol. 36, no. 12, pp. 1763–1783, 2006.

[8] J. Erochko, C. Christopoulos, R. Tremblay, and H. Choi, "Residual drift response of SMRFs and BRB frames in steel buildings designed according to ASCE 7-05," *Journal of Structural Engineering*, vol. 137, no. 5, pp. 589–599, 2011.

[9] J. Ruiz-García and E. Miranda, "Performance-based assessment of existing structures accounting for residual displacements," John A. Blume Earthquake Engineering Center, Technical Report 153, Stanford University, Stanford, CA, USA, 2005, http://blume.stanford.edu/Blume/TechnicalReports.htm.

[10] J. Ruiz-García and E. Miranda, "Evaluation of residual drift demands in regular multi-storey frames for performance-based seismic assessment," *Earthquake Engineering & Structural Dynamics*, vol. 35, no. 13, pp. 1609–1629, 2006.

[11] J. Ruiz-García and E. Miranda, "Probabilistic estimation of residual drift demands for seismic assessment of multi-story framed buildings," *Engineering Structures*, vol. 32, no. 1, pp. 11–20, 2010.

[12] S. R. Uma, S. Pampanin, and C. Christopoulos, "Development of probabilistic framework for performance-based seismic assessment of structures considering residual deformations," *Journal of Earthquake Engineering*, vol. 14, no. 7, pp. 1092–1111, 2010.

[13] U. Yazgan and A. Dazio, "Post-earthquake damage assessment using residual displacements," *Earthquake Engineering & Structural Dynamics*, vol. 41, no. 8, pp. 1257–1276, 2012.

[14] J. M. Ricles, R. Sause, M. M. Garlock, and C. Zhao, "Post-tensioned seismic-resistant connections for steel frames," *Journal of Structural Engineering*, vol. 127, no. 2, pp. 113–121, 2001.

[15] J. M. Ricles, R. Sause, S. W. Peng, and L. W. Lu, "Experimental evaluation of earthquake resistant posttensioned steel connections," *Journal of Structural Engineering*, vol. 128, no. 7, pp. 850–859, 2002.

[16] J. M. Ricles, R. Sause, Y. C. Lin, and C. Y. Seo, "Self-centering moment connections for damage-free seismic response of steel MRFs," in *Proceedings of the Structures Congress*, vol. 2010, Orlando, FL, USA, May 2010.

[17] C. Christopoulos, A. Filiatrault, and C. M. Uang, "Self-centering post-tensioned energy dissipating (PTED) steel frames for seismic regions," Report no. SSRP-2002/06, University of California, Oakland, CA, USA, 2002.

[18] C. Christopoulos and A. Filiatrault, "Seismic response of posttensioned energy dissipating moment resisting steel frames," in *Proceedings of the 12th European Conference on Earthquake Engineering*, London, UK, September 2002.

[19] C. Christopoulos, A. Filiatrault, and C. M. Uang, "Seismic demands on post-tensioned energy dissipating moment-resisting steel frames," in *Proceedings of the Steel Structures in Seismic Areas (STESSA)*, Naples, Italy, June 2003.

[20] M. M. Garlock, J. M. Ricles, and R. Sause, "Experimental studies of full-scale posttensioned steel connections," *Journal of Structural Engineering*, vol. 131, no. 3, pp. 438–448, 2005.

[21] M. M. Garlock, R. Sause, and J. M. Ricles, "Behavior and design of posttensioned steel frame systems," *Journal of Structural Engineering*, vol. 133, no. 3, pp. 389–399, 2007.

[22] M. M. Garlock, J. M. Ricles, and R. Sause, "Influence of design parameters on seismic response of post-tensioned steel MRF

systems," *Engineering Structures*, vol. 30, no. 4, pp. 1037–1047, 2008.

[23] H.-J. Kim and C. Christopoulos, "Seismic design procedure and seismic response of post-tensioned self-centering steel frames," *Earthquake Engineering & Structural Dynamics*, vol. 38, no. 3, pp. 355–376, 2009.

[24] C. C. Chung, K. C. Tsai, and W. C Yang, "Self-centering steel connection with steel bars and a discontinuous composite slab," *Earthquake Engineering & Structural Dynamics*, vol. 38, no. 4, pp. 403–422, 2009.

[25] M. Wolski, J. M. Ricles, and R. Sause, "Experimental study of self-centering beam-column connection with bottom flange friction device," *ASCE Journal of Structural Engineering*, vol. 135, no. 5, 2009.

[26] G. Tong, S. Lianglong, and Z. Guodong, "Numerical simulation of the seismic behavior of self-centering steel beam-column connections with bottom flange friction devices," *Earthquake Engineering and Engineering Vibration*, vol. 10, no. 2, pp. 229–238, 2011.

[27] Z. Zhou, X. T. He, J. Wu, C. L. Wang, and S. P. Meng, "Development of a novel self-centering buckling-restrained brace with BFRP composite tendons," *Steel and Composite Structures*, vol. 16, no. 5, pp. 491–506, 2014.

[28] Mexico City Building Code, *Normas Técnicas Complementarias para el Diseño por Sismo*, Departamento del-Distrito Federal, Mexico City, Mexico, 2004, in Spanish.

[29] J. Shen and A. Astaneh-Asl, "Hysteretic behavior of bolted-angle connections," *Journal of Constructional Steel Research*, vol. 51, no. 3, pp. 201–218, 1999.

[30] R. M. Richard, *PRCONN, Moment-Rotation Curves for Partially Restrained Connections*, RMR Design Group, Tucson, Arizona, 1993.

[31] A. Carr, *RUAUMOKO, Inelastic Dynamic Analysis Program*, University of Cantenbury, Department of Civil Engineering, Christchurch, New Zealand, 2011.

[32] A. López-Barraza, E. Bojórquez, S. E. Ruiz, and A. Reyes-Salazar, "Reduction of maximum and residual drifts on posttensioned steel frames with semirigid connections," *Advances in Materials Science and Engineering*, vol. 2013, Article ID 192484, 11 pages, 2013.

[33] E. Bojórquez and S. E. Ruiz, "Strength reduction factors for the valley of Mexico taking into account low cycle fatigue effects," in *Proceedings of the 13° World Conference on Earthquake Engineering*, Vancouver, Canada, August 2004.

[34] A. Teran-Gilmore and J. O. Jirsa, "Energy demands for seismic design against low-cycle fatigue," *Earthquake Engineering & Structural Dynamics*, vol. 36, no. 3, pp. 383–404, 2007.

[35] M. D. Trifunac and A. G. Brady, "A study of the duration of strong earthquake ground motion," *Bulletin of the Seismological Society of America*, vol. 65, no. 3, pp. 581–626, 1975.

[36] D. Vamvatsikos and C. A. Cornell, "Incremental dynamic analysis," *Earthquake Engineering and Structural Dynamics*, vol. 26, no. 3, pp. 701–716, 2002.

[37] G. G. Deierlein, "Overview of a comprehensive framework for performance earthquake assessment," Report PEER 2004/05, Pacific Earthquake Engineering Center, Berkeley, California, 2004.

[38] E. Bojórquez, A. Terán-Gilmore, S. E. Ruiz, and A. Reyes-Salazar, "Evaluation of structural reliability of steel frames: interstory drift versus plastic hysteretic energy," *Earthquake Spectra*, vol. 27, no. 3, pp. 661–682, 2011.

[39] E. Bojórquez and I. Iervolino, "Spectral shape proxies and nonlinear structural response," *Soil Dynamics and Earthquake Engineering*, vol. 31, no. 7, pp. 996–1008, 2011.

[40] J. L. Alamilla, *Reliability-based seismic design criteria for framed structures*, Ph.D. thesis, Universidad Nacional Autónoma de México, UNAM. Mexico City, Mexico, 2001, in Spanish.